

LIMITS ON CORE DRIVEN ILOT OUTBURSTS OF ASYMPTOTIC GIANT BRANCH STARS

Liron Mcley¹ and Noam Soker¹

ABSTRACT

We find that single-star mechanisms for Intermediate Luminosity Optical Transients (ILOTs; Red Transients; Red Novae) which are powered by energy release in the core of asymptotic giant branch (AGB) stars are likely to eject the entire envelope, and hence cannot explain ILOTs in AGB and similar stars. There are single-star and binary models for the powering of ILOTs, which are eruptive stars with peak luminosities between those of novae and supernovae. In single-star models the ejection of gas at velocities of $\sim 500 - 1000 \text{ km s}^{-1}$ and a possible bright ionizing flash, require a shock to propagate from the core outward. Using a self similar solution to follow the propagation of the shock through the envelope of two evolved stellar models, a $6M_{\odot}$ AGB star and an $11M_{\odot}$ yellow supergiant (YSG) star, we find that the shock that is required to explain the observed mass loss also ejects most of the envelope. We also show that for the event to have a strong ionizing flash the required energy expels most of the envelope. The removal of most of the envelope is in contradiction with observations. We conclude that single-star models for ILOTs of evolved giant stars encounter severe difficulties.

1. INTRODUCTION

The eruptive stars with peak luminosity between those of novae and supernovae (e.g. Mould et al. 1990; Rau et al. 2007; Prieto et al. 2009; Ofek et al. 2008; Botticella et al. 2009; Smith et al. 2009; Berger et al. 2009; Kulkarni & Kasliwal 2009; Mason et al. 2010; Pastorello et al. 2010; Kasliwal et al. 2011; Tylenda et al. 2013) form a heterogeneous group (Kasliwal 2011) with many enigmatic objects, and with no consensus on how to name them. We will refer to objects in this group as Intermediate-Luminosity Optical Transients (ILOTs; Berger et al. 2009), but note that Red Novae, Optical Transients, and Red Transients are also in common use, for at least some of these objects. Not only is the name for these objects not in consensus, but also the powering processes of many of

¹Department of Physics, Technion – Israel Institute of Technology, Haifa 32000 Israel; lironmc@tx.technion.ac.il, soker@physics.technion.ac.il.

them and whether they are due to binary interaction or are formed through single star evolution are debated. Since this is a heterogeneous group, it may consist of several subtypes differing by their origin and cause. The focus of this study is ILOTs whose pre-outburst objects are asymptotic giant branch (AGB) or extreme-AGB (EAGB) stars, e.g., NGC 300 OT2008-1 (NGC 300OT; Monard 2008; Bond et al. 2009; Berger et al. 2009) and SN 2008S (Arbour & Boles 2008).

There are single star models (e.g., Thompson et al. 2009; Kochanek 2011) and binary stellar models (Kashi et al. 2010; Kashi & Soker 2010b; Soker & Kashi 2011, 2012, 2013) for ILOT events harboring AGB stars. The single star mechanisms that were listed by Thompson et al. (2009) for EAGB-ILOTs are the formation of massive ONeMg WD, electron capture supernovae (ecSNe; also Botticella et al. 2009 for SN 2008S), iron core collapse supernovae (CCSNe), and outbursts of massive $\sim 10 - 15 M_{\odot}$ stars. Bond et al. (2009) derived the total radiated energy in the NGC 300OT outburst to be $\sim 10^{47}$ erg, and concluded that the NGC 300OT was an eruption of a $\sim 10 - 15 M_{\odot}$ star that cleared the surrounding dust and initiated a bipolar wind. They mention an unexplained failed SN, a binary merger, or a photospheric eruption, as possible mechanism for the NGC 300OT outburst. Berger et al. (2009) found velocities in the range of $\sim 200 - 1000 \text{ km s}^{-1}$ in the outburst of NGC 300OT, and concluded based on these, the luminosity, and an overall similarity to the ILOTs SN 2008S (Prieto et al. 2009) and M85 OT2006-1 that the outburst did not result in a complete disruption of the progenitor.

Thompson et al. (2009) mentioned that the formation of a massive ONeMg WD in the single-star scenario for EAGB-ILOTs might form a bipolar PNe. The connection between these ILOTs and bipolar PNs was mentioned also in the binary model for EAGB-ILOTs (Soker & Kashi 2012; Akashi & Soker 2013). Prieto et al. (2009) already made a connection between NGC 300OT and pre-PNe, and raised the possibility that the progenitor of NGC 300OT was of mass $< 8 M_{\odot}$. Recently more PNe were suggested to have part of their nebula ejected in an ILOT event, e.g., KJPn 8 (Boumis & Meaburn 2013). In the binary model a companion star, mostly a main sequence (MS) star, accretes part of the mass ejected by the evolved star. The gravitational energy released is channelled directly to radiation and to kinetic energy of the ejected mass. The interaction of the gas ejected in the event with previously ejected gas further increases the radiated energy. A large fraction of the ejected gas can reside in jets launched by the accreting companion star. The jets lead to the formation of a bipolar nebula, such as the Homunculus—the bipolar nebula of Eta Carinae (Kashi & Soker 2010a)—that was formed in the nineteenth century Great Eruption of Eta Carinae.

Kochanek (2011) performed a thorough analysis of the dust destruction by the shock breakout luminosity of SN 2008S and NGC 300OT, and the dust reformation. (The ‘shock breakout’ moment refers to the time when photons behind the shock expand freely to the observer. This occurs when the shock front is near the photosphere.) Kochanek (2011) concluded that the progenitors were red supergiants, and found that the required shock breakout luminosities were of order

$10^{10} L_{\odot}$, and hence the outbursts in both systems were explosive in nature. However, he could not tell whether the progenitors survived the outburst. Based on Berger et al. (2009), Smith et al. (2011) adopted an expansion speed of $v_e \simeq 560 \text{ km s}^{-1}$ for NGC 300OT. Smith et al. (2009) noted expansion speeds of about $v_e \simeq 600 - 1000 \text{ km s}^{-1}$ in SN 2008S, and estimated that it ejected $M_e \simeq 0.05 - 0.2 M_{\odot}$ in the outburst, and radiated $\sim 6 \times 10^{47} \text{ erg}$. Kochanek (2011) estimated the ejected mass and radiated energy to be $M_e > 0.05 M_{\odot}$ and $M_e > 0.25 M_{\odot}$, and $\sim 3 \times 10^{47} \text{ erg}$ and $\sim 8 \times 10^{47} \text{ erg}$, for SN 2008S and NGC 300OT, respectively.

In this study we examine the implications of such outbursts which are powered from within the stellar core. We aim at answering the following questions. (1) What are the typical energies required to account for the observed outbursts? This question is motivated by the binary-model for these outbursts where the energy comes from accretion onto a companion. In the binary model a large fraction of the liberated energy goes directly to radiation or to kinetic energy which is later channelled to radiation by wind collisions. We will find that the efficiency of the single-star model is very low. (2) Can such outbursts leave a large fraction of the envelope bound? Namely, does the star survive the outburst? This question is also motivated by the binary-model, where most of the envelope of the primary star stays bound.

In section 2 we derive the total energy that is deposited in the envelope from requirements on the ejected gas, and find that most of the envelope must be ejected to account for the velocities of the ejected mass. Our findings are similar to those of Dessart et al. (2010) who performed 1D simulations of the same process for $10 - 25 M_{\odot}$ stellar models. In section 3 we derive the energy deposited to the envelope from the required luminosity during the shock breakout, and our short summary is in section 4.

2. EJECTING HIGH VELOCITY GAS

2.1. The self similar calculation and models

We use two models calculated with the stellar evolution code MESA (Paxton et al. 2011). Both calculations were done for non-rotating stars with solar metallicity ($Z = 0.02$) at zero-age main sequence (ZAMS). The masses of $6 M_{\odot}$ and $11 M_{\odot}$ were chosen to sample the two regions below and above the critical main sequence mass for supernova explosions, $\sim 8.5 M_{\odot}$. Figs. 1 and 2 display the density and mass profiles of the two models. The AGB stellar model (Fig. 1) has a ZAMS mass of $6 M_{\odot}$. We take it at its AGB phase, at an age of $7.1 \times 10^7 \text{ yr}$, when its radius is $R_* = 675 R_{\odot}$, its luminosity is $L_* = 4.2 \times 10^4 L_{\odot}$, its effective temperature is $T_* = 3.2 \times 10^3 \text{ K}$, it has developed a $0.90 M_{\odot}$ CO core, and a $0.0048 M_{\odot}$ He mantle (outer core), and maintained a total mass of $5.98 M_{\odot}$. The yellow supergiant (YSG) stellar model (Fig. 2) has a ZAMS mass of

$11M_{\odot}$. We take it during its helium shell burning phase, at an age of 2×10^7 yr, when its radius is $R_* = 74R_{\odot}$, its luminosity is $L_* = 2.6 \times 10^4 L_{\odot}$, its effective temperature is $T_* = 8.5 \times 10^3$ K, it has developed a $1.5M_{\odot}$ CO core, the outer boundary of the helium shell is at $M = 3M_{\odot}$, and the total stellar mass is $10.9M_{\odot}$.

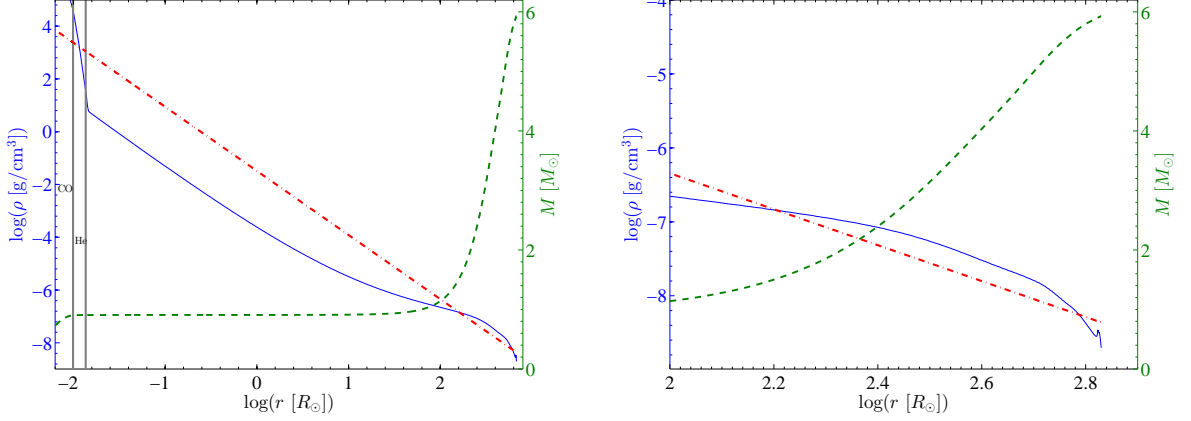


Fig. 1.— The $6M_{\odot}$ AGB model calculated with MESA. The stellar radius and luminosity are $R_* = 675R_{\odot}$ and $L_* = 4.2 \times 10^4 L_{\odot}$, respectively. The blue solid line and the green dashed line represent the density and mass profiles of the model, respectively. The right panel enlarges the outer envelope. The red dash-dot line represents our power law fitting to the outer region of the envelope as given by equation (1). We none-the-less, use this fitting for the entire envelope at $r \gtrsim 0.038R_{\odot}$ in our self-similar solution.

To facilitate an analytical self-similar solution we make a number of assumptions as follows. (1) The flow is spherically symmetric. (2) The envelope density profile can be approximated as a power law given by

$$\rho(r) = Br^{-\omega} = \begin{cases} 0.0325 \left(\frac{r}{R_{\odot}}\right)^{-17/7} \text{ g cm}^{-3}, & M_{\text{ssA}} = 5.04M_{\odot}, & \text{AGB} \\ 0.1881 \left(\frac{r}{R_{\odot}}\right)^{-17/7} \text{ g cm}^{-3}, & M_{\text{ssY}} = 8.2M_{\odot}, & \text{YSG,} \end{cases} \quad (1)$$

where M_{ss} is the total mass used in the self similar solution. This mass is somewhat larger than the envelope mass because the density profile starts at $r = 0$. The envelope masses are $M_{\text{env}}(\text{AGB}) = 5.02M_{\odot}$ and $M_{\text{env}}(\text{YSG}) = 7.9M_{\odot}$. This power-law density profile is presented with the red dash-dot line in Fig. 1 and 2. (3) The explosion energy E originated from the core region and within a time much shorter than the dynamical time in the envelope. This assumption allows us to treat the explosion as an instantaneous release of energy from the center of symmetry. (4) We assumed that radiation pressure dominates the thermal pressure so that the gas can be treated as a $\gamma = 4/3$ fluid. Although this assumption is not accurate for slow shocks, we will nevertheless present results for

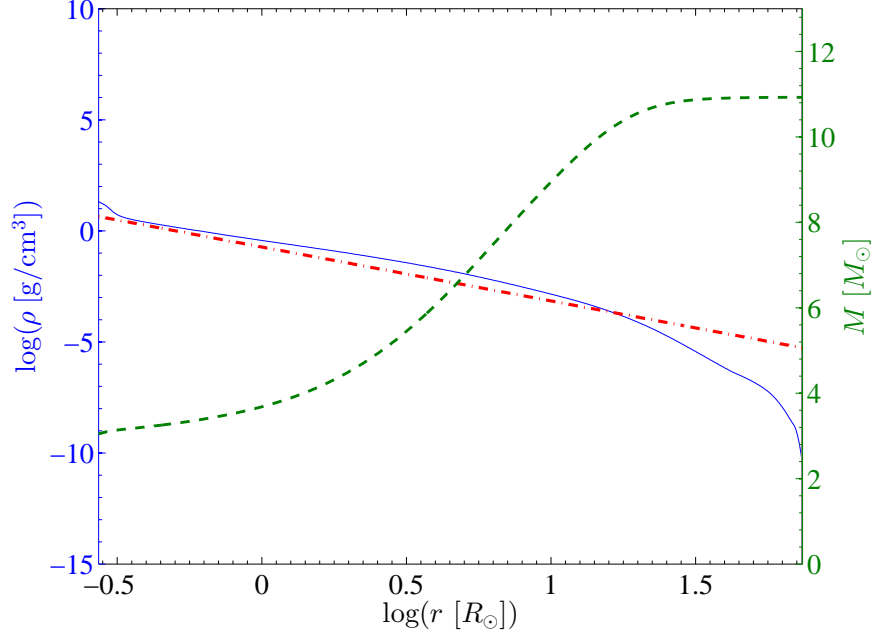


Fig. 2.— Like figure 1 but for the $11M_{\odot}$ yellow supergiant (YSG) model. The stellar radius is $R_* = 74R_{\odot}$ and its luminosity is $L_* = 2.6 \times 10^4 L_{\odot}$.

relatively slow shocks as well, where the gas pressure is higher than the radiation pressure, in order to estimate the outcome. In section 2.2 below we argue that higher values of γ will only strengthen our conclusions. (5) As the pre-shock pressure, i.e., the pressure in the envelope, is much lower than the post-shock pressure, we neglect the pre-shock pressure altogether. These assumptions imply that the solution asymptotically approaches the self similar solution for a shock wave.

We note that the power-law density profile given in equation (1) does not fit the inner part and the very outer part of the AGB envelope (Fig. 1), and the outer part of the YSG envelope (Fig. 2). We discuss the implications of the mismatch in the very outer part of the envelope in section 2.2.

We turn now to present the self similar solution to the shock. We follow the self similar solution as described by Chevalier (1976), for a shock wave travelling through an envelope with a density profile given by equation (1); see corrections in Chevalier & Soker (1989). The equations describing the post shock variables when the shock reaches R_* are,

$$v = \frac{2}{3} \frac{r}{t_{\text{end}}} , \quad e_k = \frac{1}{2} v^2, \quad (2)$$

$$\rho = 7BA^{-4/3}rt_{\text{end}}^{-8/3}, \quad (3)$$

$$P = \frac{14}{27}BA^{-4/3}r^3t_{\text{end}}^{-14/3} , \quad e_{\text{int}} = \frac{1}{\gamma - 1} \frac{P}{\rho}, \quad (4)$$

$$t_{\text{end}} = R_*^{9/7} A^{-1/2}, \quad (5)$$

where e_k and e_{int} are the specific kinetic and internal energies, respectively, t_{end} is the time when the shock reaches the radius of the star R_* , and $A = 27E/(56\pi B)$ is determined by requiring energy conservation, E being the total energy deposited in the envelope. For the solutions presented here the adiabatic index is $\gamma = 4/3$ and for $\omega = 17/7$ used here $e_k = e_{\text{int}}$ in the post-shock region. The self similar solution of the post-shock region when the shock just reaches the stellar radius is presented in Fig. 3.

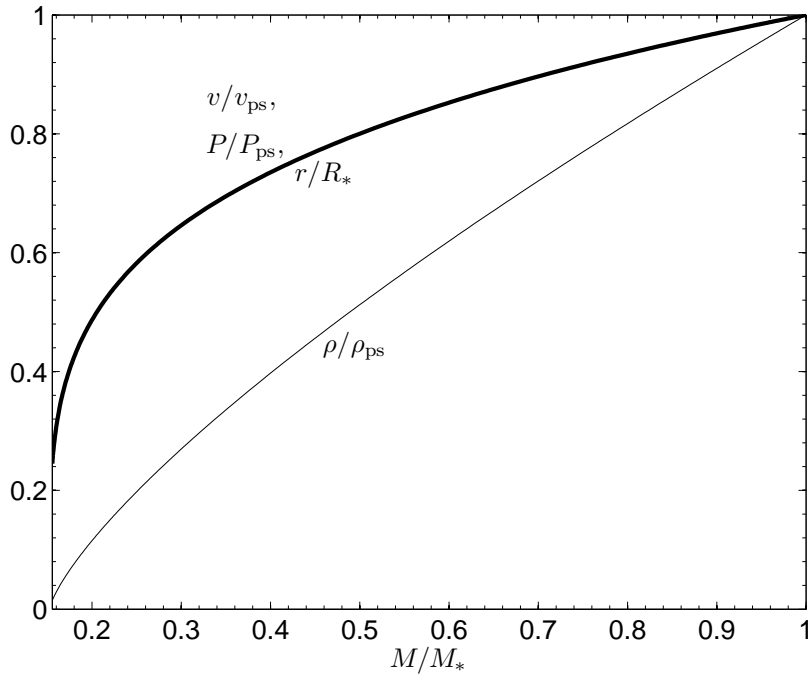


Fig. 3.— The self similar solution for $\gamma = 4/3$ and $\omega = 17/7$. The thick upper line represents the radius relative to the stellar radius, and the velocity and pressure relative to their immediate post-shock values; all these coincide. The lower line represents the density relative to its immediate post-shock value.

2.2. Results

We aim at examining how much energy is left in the envelope after the shock had passed, and in particular what fraction of the envelope has a positive energy, and hence will be ejected. The constraints on the solution from observations, as discussed in section 1, are that the shock should accelerate a mass of $M_e \sim 0.05 - 0.5M_\odot$ to velocities of $v_e \simeq 500 - 1000 \text{ km s}^{-1}$. We

note that there is a steep density gradient at the edge of the envelope, with a slope much larger than $\omega = 17/7$. In such a steep envelope a shock can accelerate gas to velocities of ~ 3 times the initial shock velocity (e.g., Tsebrenko & Soker 2013). Such an acceleration in a steep density gradient has been suggested by Humphreys et al. (2012) to explain SN 2011ht as a SN impostor. For that reason we consider a solution with shock velocities down to $v_s = 200 \text{ km s}^{-1}$. In that case the post-shock gas pressure dominates the radiation pressure, and taking the adiabatic index to be $\gamma = 4/3$ gives only a crude solution. However, this is adequate to our purposes and the other approximations, e.g., the stellar structure. Moreover, since the adiabatic index corresponds to the number of internal degrees of freedom, a larger adiabatic index, as would be the case when thermal pressure dominates, implies that more energy is available for expelling the envelope of the star.

The results of Tsebrenko & Soker (2013) show that the mass accelerated to high velocities in a steep density gradient is a small fraction of the gas mass travelling at lower velocities. For example, to eject $\sim 0.01M_\odot$ at $\sim 500 \text{ km s}^{-1}$ by post-shock gas at velocity of $\sim 250 \text{ km s}^{-1}$, we need $\gtrsim 1M_\odot$ of gas moving at $\sim 250 \text{ km s}^{-1}$.

The initial density profile of the self similar solution given in equation (1) does not include the core mass. The core mass M_{core} must be included in calculating the gravitational energy of the envelope. For that, in calculating the specific gravitational energy of a mass element at radius r , $e_G(r)$, we add the core mass M_{core} to the self-similar mass inner to r , $M_{\text{ss}}(r)$. For the same reason, our approach to the self-similar solution cannot deal with the mass that started within the core radius. We therefore present results just for the gas that started in the envelope, and the graphs below do not start at $M = 0$.

In figure 4 we present results characterized by the immediate post-shock velocity of the gas at the stellar surface v_{ps} . The energy deposited in the center in our calculation is

$$E_{\text{AGB}} = 1.68 \times 10^{49} \left(\frac{v_{\text{ps}}}{500 \text{ km s}^{-1}} \right)^2 \text{ erg} \quad (6)$$

for the AGB model and

$$E_{\text{YSG}} = 2.73 \times 10^{49} \left(\frac{v_{\text{ps}}}{500 \text{ km s}^{-1}} \right)^2 \text{ erg} \quad (7)$$

for the YSG model. These values were calculated using equations 2-5 so that matter at R_* would acquire v_{ps} when the shock reaches the stellar radius. For each of the three values of v_{ps} we show the ratio of the specific gas energy to its specific binding energy, $\xi(m) = (e_k + e_{\text{int}})/e_G$, as function of mass coordinate in the envelope. The specific binding energy is given by $e_G = G[M_{\text{core}} + M_{\text{env}}(r)]/r$, and e_k and e_{int} are the specific kinetic and internal energies. When $\xi > 1$ the gas is basically unbound. The almost horizontal shape of the $\xi(m)$ profile implies that almost the entire envelope is ejected. Our results are similar to those of Dessart et al. (2010) who performed 1D simulations of the same process for $10 - 25M_\odot$ stellar models. Dessart et al. (2010) were

interested mainly in pre-SN mass ejection, and did not refer much to surviving stars. While the explosive mass ejection by energy deposition near the core might work in major envelope removal, our results show that it cannot account for stars with repeated ILOT events, e.g., η Car, as we discuss in section 4.

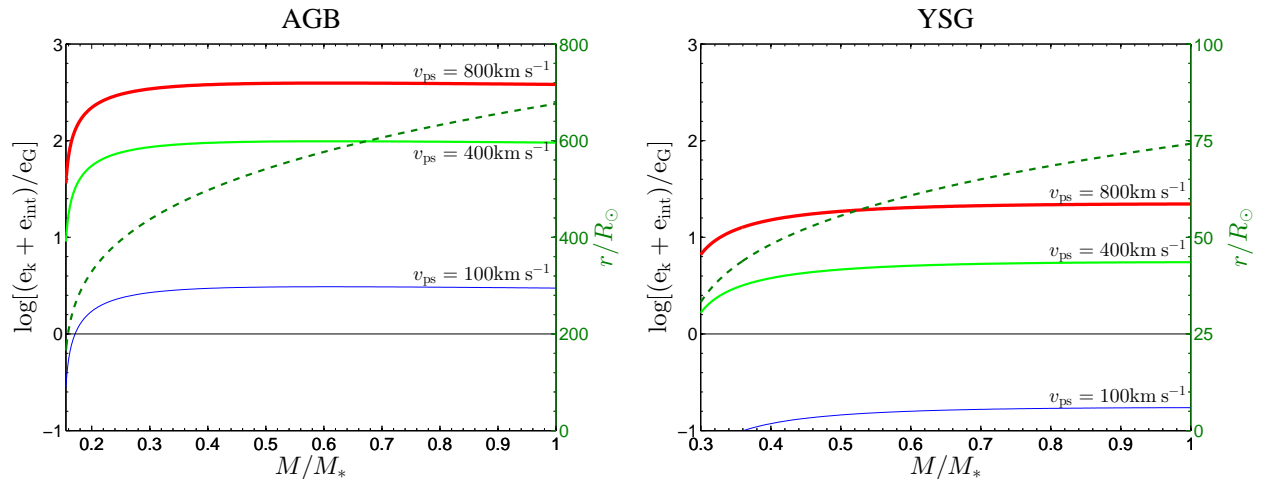


Fig. 4.— The specific energy of the post-shock stellar envelope gas relative to its binding energy, $\xi(m) = (e_k + e_{\text{int}})/e_G$, as function of mass coordinate in the envelope, and for three values of the immediate post-shock velocity at the stellar surface, $v_{\text{ps}} = 100, 400$ and 800 km s^{-1} . $\xi(m)$ is given in logarithmic scale as marked on the left axis. Results for the AGB and YSG models are presented on the left and right, respectively. The horizontal line in each panel marks $\xi = 1$. Gas elements above this line are unbound. The dashed line is the radius as function of mass in the envelope, with its scale marked on the right axis.

3. SHOCK BREAKOUT

In this section we consider the difficulty of a single star model powered by the stellar core from another direction. In his shock breakout model for NGC 300-OT and SN 2008S Kochanek (2011) requires the transient to be an explosive event, with a peak luminosity of $L_{\text{peak}} \sim 3 \times 10^{10} L_{\odot}$. The stellar radius in the model considered by Kochanek (2011) is $R_* \simeq 5 \times 10^{13} \text{ cm}$, and the duration of the breakout peak is of the order of the light crossing time $R_*/c \lesssim 10^4 \text{ s}$.

We use the parameters from Kochanek (2011) in the breakout shock solution of Katz et al. (2012), and derive the required energy for the explosion. The peak luminosity of the shock breakout is given by equation (9) of Katz et al. (2012)

$$L_{\text{peak}} \simeq 0.334\pi R_*^2 \rho_0 v_0^3, \quad (8)$$

while the typical duration is (their eq. 5)

$$t_0 \simeq \frac{c}{\kappa \rho_0 v_0^2}. \quad (9)$$

Here v_0 is the shock velocity, ρ_0 is the pre-shock density, and κ is the opacity. Last two equations give

$$L_{\text{peak}} \simeq 4R_*^2 v_0 c (\kappa t_0)^{-1}. \quad (10)$$

Their derivation gives for a $5M_\odot$ envelope (their eq. 14)

$$v_0 \simeq 2000 \left(\frac{E_{\text{in}}}{10^{50} \text{ erg}} \right)^{0.5} \text{ km s}^{-1}, \quad (11)$$

where E_{in} is the total energy injected into the envelope in the explosion. From equations (10) and (11) and for Thomson scattering opacity we derive

$$L_{\text{peak}} \simeq 4 \times 10^{10} \left(\frac{E_{\text{in}}}{10^{50} \text{ erg}} \right)^{0.5} \left(\frac{t_0}{1000 \text{ s}} \right)^{-1} \left(\frac{R}{5 \times 10^{13} \text{ cm}} \right)^2 L_\odot. \quad (12)$$

We conclude that in order to have an outburst with the luminosity required by the model of Kochanek (2011), the explosion energy should be $E_{\text{in}} \sim 10^{50} \text{ erg}$. This energy is much larger than the binding energy of the envelope of EAGB stars, resulting in a massive mass ejection from the envelope. Basically, the entire envelope becomes unbound by the outburst.

4. IMPLICATIONS AND SUMMARY

We used a self-similar solution to study energy deposition within a short time scale near evolved stellar cores. This process is at the heart of some single-star models for the outburst of intermediate luminosity optical transients (ILOTs). The two stellar models and our approximated power-law density profiles are shown in Fig. 1 and 2. A shock runs through the stellar envelope, as depicted in Fig. 3. In Fig. 4 we present the ratio of gas energy to its binding energy as a function of mass coordinate in the envelope $\xi(m)$, when the shock front reaches the stellar surface.

There is one clear implication from the behavior of $\xi(m)$: To eject a small amount of mass from the surface at more than the escape speed, implies that almost the entire envelope is lost. Our results are similar to those of Dessart et al. (2010) who were aiming indeed at explaining massive envelope removal. Namely, the star is seriously disrupted, it cannot return to its previous structure, and also cannot experience repeated ILOT events.

Very small amounts of gas, below those required by the observations described in section 1, can be ejected because of the steep density profile on the stellar surface. Typically, at velocities of

three times the shock velocity (e.g., Tsebrenko & Soker 2013). The results of Tsebrenko & Soker (2013) show that the mass accelerated to high velocities in a steep density gradient is a very small fraction of the gas mass at lower velocities. For example, to eject $\sim 0.1M_{\odot}$ at $\sim 500 \text{ km s}^{-1}$ by post-shock gas at velocity of $\sim 250 \text{ km s}^{-1}$, we need $\gtrsim 10M_{\odot}$ of gas moving at $\sim 250 \text{ km s}^{-1}$. Again, this implies that most of the envelope is ejected.

In section 3 we derived the energy that is required to be deposited in the core to obtain the luminosity in the shock breakout model of Kochanek (2011) for the ILOTs NGC 300-OT and SN 2008S. We find that the required energy is $\sim 10^{50}$ erg, as given by equation (12). Again, the entire envelope is lost by such an energy deposition. This strengthens the results we have found in section 2.2. Namely, to account for energetic ILOTs by energy deposited near the core, the entire envelope is lost. This is in contradiction to observations presented in section 1, and to some ILOTs that seem to return to their previous stage, e.g., η Carinae after the Great Eruption (Davidson & Humphreys 1997) and the first two outbursts of SN 2009ip (Mauerhan et al. 2013). However, if it turns out that in an ILOT most of the envelope is ejected, then energy deposition from the core is required, and indeed can account for such a process (Dessart et al. 2010).

The problems we find with models based on a shock running through the envelope, as required for a shock breakout UV flash, do not apply to the case where the core excites waves propagating throughout the envelope, as in the wave-driven mass loss in the SN progenitor mechanism proposed by Quataert & Shiode (2012) and Shiode & Quataert (2014). The wave-driven mass loss was proposed to account for heavy mass loss years before core collapse SNe. Soker (2013) raised the possibility that the pre-explosion outburst (PEO) of the type II_n supernova 2010mc (PTF 10tel; Ofek et al. 2013a) was energized by mass accretion onto an O main-sequence stellar companion, and the ejecta had a bipolar structure. Soker (2013) conjectured that all Type II_n supernovae owe their dense circumstellar gas to binary interaction. Humphreys et al. (2012) already mentioned that SN 2011ht, as well as other types of II_n SNe, can be explained if they are strongly non-spherical. It was recently proposed (Fransson et al. 2014) that the massive ejecta (Ofek et al. 2013b) of the PEO of SN 2010jl has a bipolar structure. If holds, a bipolar structure strengthens the binary conjecture of Soker (2013). The problems we find in some single-star models, further strengthen the binary model for ILOTs (Kashi & Soker 2010b).

We thank the referee, Kris Davidson, for his helpful comments. This research was supported by the Asher Fund for Space Research at the Technion, The US - Israel Binational Science Foundation, and a generous grant from the president of the Technion Prof. Peretz Lavie.

REFERENCES

Akashi, M., & Soker, N. 2013, MNRAS, 2394

- Arbour, R., & Boles, T. 2008, CBET, 1234, 1
- Berger, E., Soderberg, A. M., Chevalier, R. A., et al. 2009, ApJ, 699, 1850
- Bond, H. E., Bedin, L. R., Bonanos, A. Z., Humphreys, R. M., Monard, L. A. G. B., Prieto, J. L., & Walter, F. M. 2009, ApJ, 695, L154
- Botticella, M. T., Pastorello, A., Smartt, S. J., et al. 2009, MNRAS, 398, 1041
- Boumis, P., & Meaburn, J. 2013, MNRAS, 430, 3397
- Chevalier, R. A. 1976, ApJ, 207, 872
- Chevalier, R. A., & Soker, N. 1989, ApJ, 341, 867
- Davidson, K., & Humphreys, R. M. 1997, ARA&A, 35, 1
- Dessart, L., Livne, E., & Waldman, R. 2010, MNRAS, 405, 2113
- Fransson, C., Ergon, M., Challis, P. J., et al. 2014, arXiv:1312.6617
- Humphreys, R. M., Davidson, K., Jones, T. J., Pogge, R. W., Grammer, S. H., Prieto, J. L., & Pritchard, T. A. 2012, ApJ, 760, 93
- Kashi, A., Frankowski, A., & Soker, N. 2010, ApJ, 709, L11
- Kashi, A., & Soker, N. 2010a, ApJ, 723, 602
- Kashi, A., & Soker, N. 2010b, (arXiv:1011.1222)
- Kasliwal, M. M. 2011, Bulletin of the Astronomical Society of India, 39, 375
- Kasliwal, M. M., et al. 2011, ApJ, 730, 134
- Katz, B., Sapir, N., & Waxman, E. 2012, ApJ, 747, 147
- Kochanek, C. S. 2011, ApJ, 741, 37
- Kulkarni, S. R., & Kasliwal, M. M. 2009, astro2010: The Astronomy and Astrophysics Decadal Survey, 2010, 165
- Mason, E., Diaz, M., Williams, R. E., Preston, G., & Bensby, T. 2010, A&A, 516, A108
- Mauerhan, J. C., Smith, N., Filippenko, A. V., et al. 2013, MNRAS, 430, 1801
- Monard, L. A. G. 2008, IAU Circ., 8946, 1

- Mould, J., et al. 1990, *ApJ*, 353, L35
- Ofek, E. O., Kulkarni, S. R., Rau, A., et al. 2008, *ApJ*, 674, 447
- Ofek, E. O., Sullivan, M., Cenko, S. B., et al. 2013a, *Nature*, 494, 65
- Ofek, E. O., Zoglauer, A., Boggs, S. E., et al. 2013b, *arXiv:1307.2247*
- Pastorello, A., et al. 2010, *MNRAS*, 408, 181
- Paxton, B., Bildsten, L., Dotter, A., et al. 2011, *ApJS*, 192, 3
- Prieto, J. L., Sellgren, K., Thompson, T. A., & Kochanek, C. S. 2009, *ApJ*, 705, 1425
- Quataert, E., & Shiode, J. 2012, *MNRAS*, 423, L92
- Rau, A., Kulkarni, S. R., Ofek, E. O., & Yan, L. 2007, *ApJ*, 659, 1536
- Shiode, J. H., & Quataert, E. 2014, *ApJ*, 780, 96
- Smith, N., Ganeshalingam, M., Chornock, R., et al. 2009, *ApJ*, 697, L49
- Smith, N., Li, W., Silverman, J. M., Ganeshalingam, M., & Filippenko, A. V. 2011, *MNRAS*, 415, 773
- Soker, N. 2013, *arXiv:1302.5037*
- Soker, N., & Kashi, A. 2011 (*arXiv:1107.3454*)
- Soker, N., & Kashi, A. 2012, *ApJ*, 746, 100
- Soker, N., & Kashi, A. 2013, *ApJ*, 764, L6
- Thompson, T. A., Prieto, J. L., Stanek, K. Z., Kistler, M. D., Beacom, J. F., Kochanek, C. S. 2009, *ApJ*, 705, 1364
- Tsebrenko, D., & Soker, N. 2013, *ApJ*, 777, L35
- Tylenda, R., Kaminski, T., Udalski, A., et al. 2013, *arXiv:1304.1694*